

## **CHAPTER 1**

# **Influence of Intervening Mismatches on Long-Range Guanine Oxidation**

Adapted from Bhattacharya, P. K.; Barton, J. K. (2001) *Journal of the American Chemical Society*, 123, 8649-8656.

## Abstract

A systematic investigation of the efficiency of oxidative damage at guanine residues through long-range charge transport was carried out as a function of intervening base mismatches. A series of DNA oligonucleotides were synthesized that incorporate a ruthenium intercalator linked covalently to the 5' terminus of one strand and containing two 5'-GG-3' sites in the complementary strand. Single base mismatches were introduced between the two guanine doublet steps, and the efficiency of transport through the mismatches was determined through measurements of the ratio of oxidative damage at the guanine doublets distal versus proximal to the intercalated ruthenium oxidant. Differing relative extents of guanine oxidation were observed for the different mismatches. The damage ratio of oxidation at the distal versus proximal site for the duplexes containing different mismatches varies in the order GC ~ GG ~ GT ~ GA > AA > CC ~ TT ~ CA ~ CT. For all assemblies, damage found with the  $\Delta$ -Ru diastereomer was found to be greater than with the  $\Lambda$ -diastereomer. The extent of distal/proximal guanine oxidation in different mismatch-containing duplexes was compared with the helical stability of the duplexes, electrochemical data for intercalator reduction on different mismatch-containing DNA films, and base-pair lifetimes for oligomers containing the different mismatches derived from  $^1\text{H}$  NMR measurements of the imino proton exchange rates. While a clear correlation is evident both with helix stability and electrochemical data monitoring reduction of an intercalator through DNA films, damage ratios correlate most closely with base-pair lifetimes. Competitive hole trapping at the mismatch site does not appear to be a key factor governing the efficiency of transport through the mismatch. These results underscore the importance of base dynamics in modulating long-range charge transport through the DNA base-pair stack.

## Introduction

The DNA double helix is a remarkable molecular assembly for examining how a  $\pi$ -stacked array mediates charge transport. Theoretical (1) and experimental studies (2) have demonstrated that 5'-GG-3' sequences in DNA are "hot spots" for oxidative damage. Preferential damage to guanine can be rationalized by comparing the oxidation potential of free nucleosides in aqueous solution. The oxidation potential of dG measured by pulse radiolysis is 1.3 V versus NHE, lower than those of dA (1.4 V), dC (1.6 V), and dT (1.7 V) (3). In DNA, the potentials also appear to be dependent on stacking with neighboring bases. *Ab initio* molecular orbital calculations indicate that the ionization potential of stacked pairs of DNA bases is lowest for 5'-GG-3', with the bulk of the HOMO located on the 5'-guanine (1).

Migration of charge through DNA has been demonstrated in systems in which DNA acts both as a bridge for charge transport between donor and acceptor molecules and as a reactant (4-10). Although data and mechanistic conclusions about DNA-mediated charge transport vary widely among these studies, it is clear that charge transport through DNA is dependent upon the stacking of the donor and acceptor molecules within the base stack and also upon the intervening  $\pi$ -stacked conformation.

The first demonstration of long-range oxidative damage at the 5'-G of 5'-GG-3' doublets, now taken as a hallmark of damage owing to electron transfer chemistry, was carried out using DNA assemblies containing a tethered phenanthrenequinone diimine ( $\phi$ ) complex of rhodium, a potent photooxidant and tightly bound metallointercalator (2). This oxidation occurs even when the rhodium complex is covalently tethered to one end of the DNA assembly at a distance of 60 base pairs (200 Å) (5). This oxidation from a remote site is sensitive to the stacking of the intercalator within the helix, because the right-handed ( $\Delta$ ) isomer, which fits more deeply into the right-handed DNA helix, is more efficient in oxidizing guanine than is the left-handed ( $\Lambda$ ) isomer. Long-range

oxidation is sensitive to disturbances in the intervening stack, as was evident in studies in which intervening bulges were incorporated in the assemblies (6); larger bulges which significantly disrupt the  $\pi$ -stack (for example, a 5'-ATA-3' bulge) diminish the distal oxidation significantly. Long-range oxidative damage to DNA is also highly sensitive to protein-induced DNA distortions (7), as was evident in studies using the base-flipping methyltransferase protein *HhaI*.

Since these studies, long-range oxidative DNA damage has been demonstrated with a range of photooxidants (8), like modified anthraquinones, modified stilbenes, naphthalimides, and sugar radicals. It has, for example, also been demonstrated that ground-state ruthenium(III) generated *in situ* can oxidize guanine doublets over a comparable distance (5,9). When the guanine doublets are replaced by single guanines, the damage becomes equally distributed over all of the guanine bases, the sites of equivalent oxidation potential. Guanine oxidation by Ru(III) was also found to be sensitive to an intervening mismatch (9), as shown by the diminution of distal guanine damage when a thermodynamically destabilizing GT mismatch is present between the 5'-GG-3' site and the metal but not when a less disruptive GA mismatch was present.

The influence of mismatches on long-distance guanine damage through DNA was also recently examined by Giese and Wessely, who found a strong decrease in charge transport in DNA oligomers in which a mismatch was introduced at a GC base pair (10). They attributed this decrease to a change in trapping of the guanine radical in the presence of the mismatch; specifically, they proposed that there is an increased water accessibility at the mismatch site, so that the trapping of guanine cation radical by water competes with the charge transfer through the DNA duplex. In another study (11), the rate constants for guanine oxidation at mismatches in DNA oligomers by Ru(bpy)<sub>3</sub><sup>3+</sup> were measured electrochemically. The oxidation rate constants followed the trend

G(single strand) > GA > GG > GT > GC; this variation in rate constants was reasonably attributed to the changes in accessibility to  $\text{Ru}(\text{bpy})_3^{3+}$  around the mismatch site.

Electrochemical detection of mismatches has also been demonstrated in experiments that depend on DNA-mediated charge transport rather than accessibility to an oxidant. In these experiments, the reduction of an intercalator bound to a DNA-modified electrode was found to be significantly attenuated in the presence of an intervening CA mismatch (12). Importantly, mismatch detection was found to be independent of DNA sequence context. Furthermore, the detection of different DNA lesions was accomplished. This methodology may become useful as a diagnostic sensor for genetic analysis, because, by coupling the reduction of the DNA-bound intercalator to an electrocatalytic cycle, using DNA-modified electrodes, all mismatches can be sensitively detected (13). We attribute this sensitive detection of mismatches in the DNA films not to solvent accessibility but rather to the exquisite sensitivity of DNA charge transport to perturbations in base stacking.

Different mismatches bring about different stacking and orientational properties of the base pairs because of their different geometrical dispositions, stacking propensities, and hydrogen bonding abilities and these stacking differences are not static, but they vary depending upon their characteristic lifetimes. Remarkably, few studies have been carried out that systematically describe dynamical properties of mismatches. For well-matched base pairs, studies of base-pair opening dynamics have revealed information about sequence dependent properties of the DNA duplex, such as flexibility, stability, and groove width (14). The base-pair lifetimes are strongly dependent on the sequence context, but generally, AT base-pair lifetimes have been found to be in the range 1-5 ms at 15 °C, and for isolated GC base pairs, they are about 10 times longer (15). However, tracts of GC base pairs (sequences containing guanine and cytosine and at least four bases long) show unusually rapid dynamics in the 1-5 ms range (16). In AT tracts, base-pair

lifetimes longer than 100 ms were observed (15a), consistent with the great rigidity associated with bent DNA. However, dynamical changes occur on much faster time scales as well, as evident by studies of fluorescence anisotropies in the presence of mismatches (17). In an effort to begin to characterize mismatch structure and dynamics, we have also carried out  $^1\text{H}$  NMR measurements of imino proton exchange and, hence, of base-pair lifetimes in DNA oligonucleotides containing GG, TT, AA, and CC mismatches (18).

Here we systematically examine the effect of intervening mismatches on long-range guanine oxidation in DNA assemblies containing a ruthenium intercalator as the tethered oxidant. These data are compared with measurements of helical stability in the presence of DNA mismatches, with electrochemical measurements of charge transport through DNA duplexes containing mismatches, as well as with studies of the base-pair lifetimes of oligomers containing mismatches. These comparisons reveal a clear correlation between long-range guanine oxidation and each of these parameters, and in particular with the base-pair dynamics associated with a DNA mismatch.

## Experimental Section

**Oligonucleotide Preparation.** Oligonucleotides (22 base pairs) were synthesized using standard phosphoramidite chemistry on an Applied Biosystems 392 DNA synthesizer with a dimethoxy trityl protective group on the 5' end (19). Oligonucleotides were purified on a reversed-phase Rainin Dynamax  $\text{C}_{18}$  column on a Waters HPLC and deprotected by incubation in 80% acetic acid for 15 min. After deprotection, the oligonucleotides were purified again by HPLC. The concentration of the oligonucleotides was determined by UV-visible spectroscopy (Beckman DU 7400), using the extinction coefficients estimated for single-stranded DNA,  $\epsilon(260 \text{ nm}, \text{M}^{-1} \text{cm}^{-1})$ : adenine (A) = 15 400, guanine (G) = 11 500, cytosine (C) = 7400, and thymine (T) =

8700. Single strands were mixed with equimolar amounts of the complementary strand and were annealed in a Perkin-Elmer Cetus Thermal Cycler by gradual cooling from 90 °C to ambient temperature in 90 min. Circular dichroism (CD) spectra were recorded on a JASCO J-500C spectropolarimeter.

**Synthesis of the Ruthenium Complex.** Ru(phen)(bpy')(dppz)<sup>2+</sup> (phen = 1,10 phenanthroline; bpy' = 4-butyric acid-4'-methylbipyridine; dppz = dipyrido[3,2-a:2',3'-c]phenazine) was prepared according to published procedures (20).

**Preparation of Ruthenium-Modified Oligonucleotides.** Ruthenium-tethered 22-base-pair oligonucleotides were prepared according to published procedures (9,21) and purified on a reversed-phase Rainin Dynamax C<sub>18</sub> column on a Hewlett-Packard 1050 HPLC. The diastereomeric strands were isolated and numbered according to the order of elution, and the absolute configuration around the metal center was determined by circular dichroism based on the stereochemistry of the metal center (22). The ruthenium-conjugated oligonucleotides were quantitated using the following extinction coefficient: for Ru(phen)(bpy')(dppz)<sup>2+</sup> modified oligonucleotides,  $\epsilon(432 \text{ nm}, \text{M}^{-1} \text{ cm}^{-1}) = 19,000$ .

**Oxidation with Ruthenium-Modified Oligonucleotides.** Oligonucleotides were radioactively labeled by incubation with  $\gamma$ -<sup>32</sup>P-ATP and T4 polynucleotide kinase as per standard protocol (23). The labeled strands were annealed with complementary unlabeled metalated single strands at a concentration of 2.5  $\mu\text{M}$  (strands) in 35 mM Tris HCl, pH 8.0, 5 mM NaCl, as described. 25  $\mu\text{L}$  aliquots were irradiated at 432 nm for 5 min on a 1000 W Hanovia Hg-Xe arc lamp equipped with a monochromator in the presence of 25  $\mu\text{M}$  methyl viologen quencher. The flash-quench methodology was employed for oxidizing guanine within the DNA duplex (9,24). Control aliquots were not irradiated but were otherwise treated similarly to those samples which were irradiated. All samples were treated with 10% piperidine for 30 min at 90 °C, lyophilized, and then analyzed by

PAGE in a 12% denaturing gel. Cleavage of the labeled strand was measured by phosphorimager using ImageQuant, v3.3 (Molecular Dynamics). The levels of oxidation at individual guanine bases in the distal and proximal sites were determined by measuring the intensity of the band corresponding to that base as a fraction of the intensity of the whole lane, using phosphorimager. The fractional intensity of the corresponding band in the control lane was subtracted out to account for background levels of damage. The ratio of the intensity at the distal site normalized to that at the proximal site gives the distal/proximal guanine oxidation ratio.

**Melting Temperature Experiments.** The melting temperatures ( $T_m$ ) of the oligonucleotides were determined from absorbance versus temperature curves measured at 260 nm on a Beckman DU 7400 UV-visible spectrophotometer. The 10  $\mu$ M duplex was tested in a buffer of 15 mM NaCl and 5 mM sodium phosphate (pH 7.0).

## Results and Discussion

**Sequence Design and Strategy.** The general sequence used in the guanine oxidation experiment is given in Figure 1. The 22-base-pair assembly contains two guanine doublets separated by nine bases, with the first guanine doublet three base pairs away from the predominant intercalation site. Mismatches were introduced between the two guanine doublets. Sixteen combinations of the base pairs and mispairs are possible, and all corresponding assemblies were constructed. All the mismatches have the identical flanking sequence (AXT/TYA). Each guanine doublet is flanked by the same

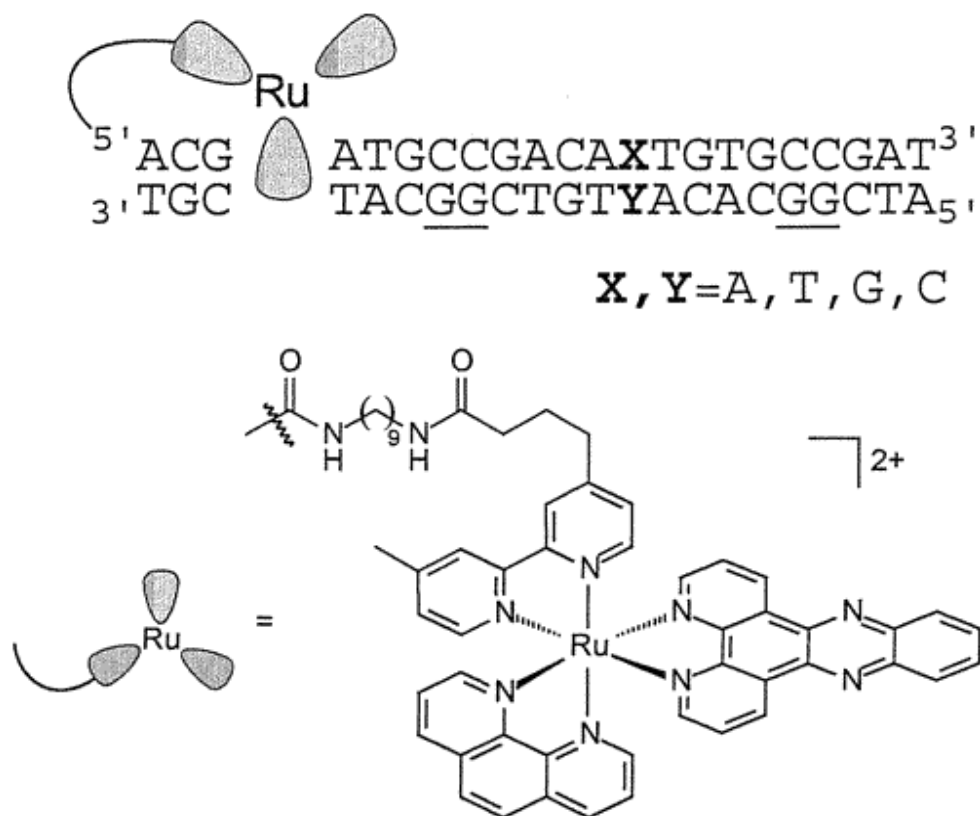


**Figure 1.1.** Schematic illustration of the ruthenium-conjugated 22 mer DNA duplex constructs used in the study containing intervening mismatch. The 5' end of the duplex is tethered to the trisheteroleptic metalointercalator,  $[\text{Ru}(\text{bpy}')(\text{dppz})(\text{phen})]^{2+}$ , by a nine-carbon linker from the appended arm of the  $\text{bpy}'$  ligand. The assembly contains two guanine doublets separated by nine bases with mismatches (XY) introduced between the two guanine doublets. All the mismatches have the identical flanking sequence 5'-AXT-3'. Sixteen combinations of the base pairs and mispairs are possible, and all the corresponding assemblies were constructed. For each mismatched assembly, as well as for the well matched sequences, the four ruthenium diastereomers were separately examined.

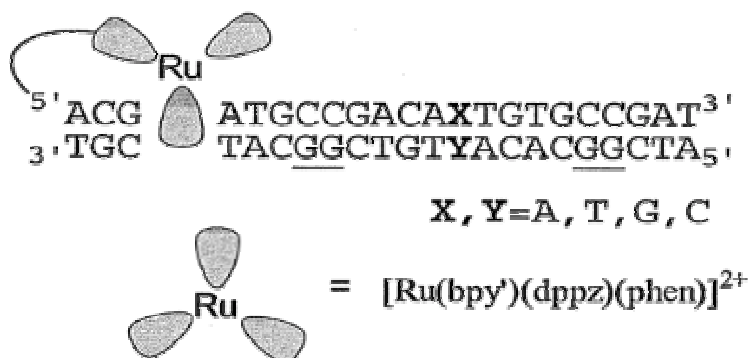
base (cytosine) on its 3' and 5' sides, and the guanine doublets are located on the strand complementary to that containing the tethered metallointercalator. For each mismatched assembly, as well as for the well-matched sequences, the four ruthenium diastereomers were separately examined.

Oxidation was carried out using the flash-quench technique (9, 24) developed earlier to study long-range electron-transfer reactions in proteins (25). In this method, the ruthenium(III) intercalator, which serves as the oxidant, is generated in situ upon photolysis of the ruthenium(II) species in the presence of a diffusional quencher such as methyl viologen. Once generated, ruthenium(III) can oxidize guanines from a distance in the DNA duplex. Transient absorption spectroscopy reveals that the guanine radical cation deprotonates on a fast time scale to afford the neutral radical which reacts on the millisecond time scale with water and/or oxygen to yield irreversible oxidative products (24). Many of these products are revealed as strand breaks upon treating the DNA with hot piperidine (9).

**Oxidation of DNA Assemblies Containing Mismatches.** Oxidation at the 5' guanines of both the distal and proximal doublets in all of the assemblies was observed after irradiation at 432 nm in the presence of the quencher methyl viologen. Figure 2 shows a typical phosphoimagery result after denaturing electrophoresis of the DNA fragments. The value of the distal/proximal guanine oxidation ratio is found to be different for different mismatches. Figure 3 summarizes the results for one  $\Delta$ -Ru diastereomer, and Table 1 provides quantitation of the data for different trials.



**Table 1.1.** The Distal/Proximal Guanine Oxidation Data<sup>a</sup> for Duplexes Shown below Containing Intervening Mismatch (XY) with the Appended  $\Delta$ -Isomer of  $[\text{Ru}(\text{bpy}')(\text{dppz})(\text{phen})]^{2+}$



base pair <sup>b</sup>	distal/proximal oxidation <sup>c</sup>	base pair	distal/proximal oxidation
TA* <sup>d</sup>	$0.23 \pm 0.04^e$	GA	$1.34 \pm 0.44$
AT*	$0.23 \pm 0.07$	AG	$1.48 \pm 0.49$
CG*	$2.05 \pm 0.44$	TG	$1.52 \pm 0.51$
GC*	$1.32 \pm 0.30$	GT	$1.36 \pm 0.44$
CC	$0.30 \pm 0.11$	CA	$0.45 \pm 0.21$
GG	$1.72 \pm 0.25$	AC	$0.27 \pm 0.09$
AA	$0.72 \pm 0.15$	TC	$0.15 \pm 0.02$
TT	$0.19 \pm 0.09$	CT	$0.28 \pm 0.13$

<sup>a</sup> Samples were prepared, irradiated, and analyzed using PAGE as described in the Experimental Section. <sup>b</sup> Designation of XY as shown in assembly. <sup>c</sup> The ratio of the percent cleavage at the distal guanine doublet to that at the proximal doublet was determined using phosphorimager. <sup>d</sup> XY\* corresponds to Watson-Crick paired sequence. <sup>e</sup> Shown are the mean and standard deviation of the proximal/distal ratio based on at least three trials.

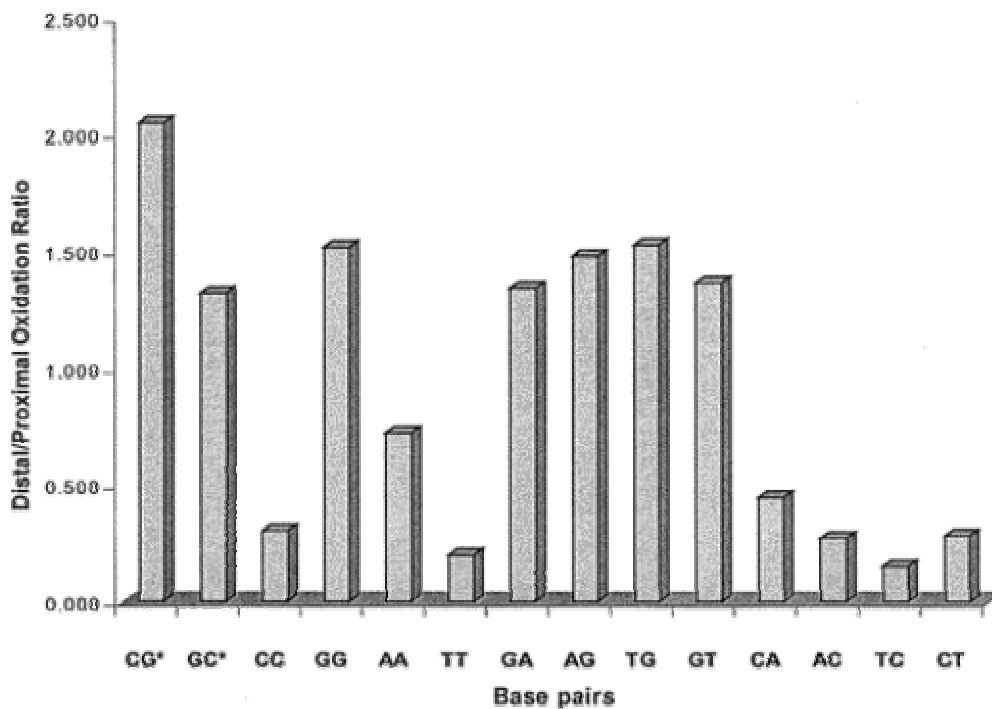


**Figure 1.3.** Bar chart showing the ratio of distal/proximal damage as a function of different intervening mismatches for the  $\Delta$ -diastereomer of  $[\text{Ru}(\text{bpy}')(\text{dppz})(\text{phen})]^{2+}$ . The damage ratio of oxidation at the distal versus the proximal site for the duplexes containing different mismatches varies in the order:  $\text{GC} \sim \text{GG} \sim \text{GT} \sim \text{GA} > \text{AA} > \text{CC} \sim \text{TT} \sim \text{CA} \sim \text{CT}$ .

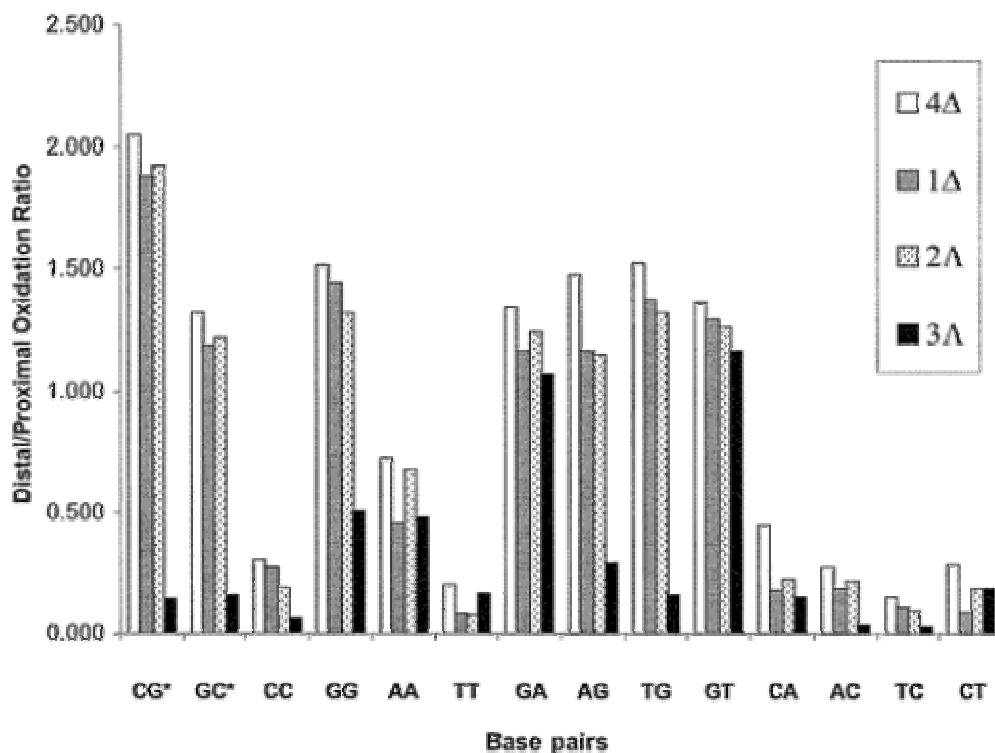


**Figure 1.4.** A comparative bar chart of distal/proximal guanine oxidation ratios as a function of different intervening mismatches for all the four diastereomers of  $[\text{Ru}(\text{bpy}')(\text{dppz})(\text{phen})]^{2+}$ . Ratios were determined as described in the Experimental section. The efficiency of oxidation depended on the diastereomer of the metal-conjugated strand. The general order of reactivity is  $4\Delta > 1\Delta \sim 2\Delta > 3\Delta$ , where the number denotes the order these isomers elute from the HPLC column. The order is consistent with previous studies (5) indicating that the right-handed isomers are better able to fit into the major groove and intercalate into the  $\pi$ -stack of the DNA duplex.

It is seen that the purine-purine mismatches (GG, GA, AG, AA) all have fairly high distal/proximal guanine oxidation ratios. Among the purine-purine mismatches, the lowest ratio is seen with AA. Interestingly, all base pairs containing G yield high ratios, even the GT wobble pair. In contrast, the pyrimidine-pyrimidine mismatch-containing duplexes show lower distal/proximal guanine oxidation ratios. The damage ratios do not, however, simply reflect differences in oxidation potentials at the mismatch site; the AC mismatch-containing duplex, for example, yields a very low ratio. Notably, small differences also are evident depending upon the strand disposition, for example, AC versus CA. In the case of B-DNA, over this distance regime, charge transport is expected to be largely intrastrand (4g).

Stacking of the photooxidant within the DNA duplex also affects the damage ratio. Oxidation ratios are seen to differ among the four diastereomeric metal-conjugated strands (Figure 4), with the  $4\Delta$  isomer yielding the highest extent of oxidation and the  $3\Lambda$  isomer yielding the lowest values. The order of reactivity,  $4\Delta > 1\Delta \sim 2\Lambda > 3\Lambda$ , seen here confirms results seen earlier (5). The results are consistent with the right-handed  $\Delta$ -isomers being better able to fit into the right-handed helix and intercalate into the DNA  $\pi$ -stack (26).

We also quantitated the damage directly at the mispair for those mismatches containing guanine. The damage directly at the site varies in the order  $GA > GG > GT > GC$ . In no case, however, does this damage represent more than 2.5% of damage across the duplex. Hence, no difference in the trend of distal/proximal oxidation ratios in the guanine-containing mismatches is observed, if the damage at the mismatch site is taken into consideration. On the basis of this quantitation alone, it seems difficult to argue that trapping of the guanine radical at this mismatched site is significantly competitive with hole transport. Instead, the fact that some damage is apparent at these sites suggests that the presence of the mismatch may alter the redox potential of the guanine at the site (9).

It is noteworthy that a small amount of damage is observed also at the guanine located 3' to each mismatched base. A similar finding was obtained previously in studies with GA mismatches (9) and thymine dimer lesions (4n). This result is interesting, because it suggests that if charge migration through DNA occurs physiologically, mismatches and other disturbances in the helical stack have the potential to hinder the migration of charge through DNA, leading to the buildup of damage around the disturbed site.

**Comparisons with Other Studies.** As described previously, Geise and co-workers have recently reported a limited study of the effect of intervening mismatches on long-range guanine oxidation (10), and they concluded that any attenuation in long-range oxidation arose from a competition between trapping of a guanine radical at the mismatch site versus hole transport; at a guanine-containing mismatch, the guanine radical would be more accessible and, hence, easier to trap. The oxidant used as well as assemblies in which charge transport is measured differ from those described here, and that may lead to some differences between the two systems with respect to relative yields. Nonetheless, the proposed explanation of Geise and co-workers for attenuation of yield in the presence of intervening mismatches is clearly invalid here. It is evident from the results that mismatches that do not contain guanines, in fact, lead to the largest attenuation in the yield of long-range guanine oxidation. Guanine-containing mismatches instead cause at most only small perturbations in long-range charge transport. Therefore, competitive hole trapping at the mismatch site does not appear to be a key factor governing the efficiency of electron transport. Solvent accessibility is clearly, however, a more important issue governing studies of guanine oxidation in mismatches by solution-borne ruthenium (11).

One could also argue that G at the mismatch site, through a base hopping mechanism (8), increases long-range oxidative damage compared to the oxidation seen

with intervening mismatches that lack G. Surely, the overall energetics of the bridge is not changed with these substitutions, because only one base in a nine-base bridge is altered. We had observed earlier, moreover, that insertion of guanines in repetitive AT tracts does not increase long-range oxidative damage (27). Furthermore, we observe similar variations with intervening mismatches using reductive chemistry, where the presence of the easily oxidized G is not advantageous (*vide infra*) (12).

**Sequence-Dependent Oxidation of DNA Assemblies Containing Matched Sequences.** We also examined the distal/proximal ratios in the analogous sequence without mismatches. These results indicate further that the greater "accessibility" associated with a mismatch is not the determining factor. We compared damage ratios for the GC matched pairs with AT matched pairs, and as is evident also in Table 1, these ratios essentially bracket values for the mismatched sequences. The highest ratios are seen with GC matched pairs. Here too, significant differences are evident even between GC and CG matched pairs. Importantly, the AT matched sequences yield extremely low damage ratios.

It is noteworthy that in these oligomers the sequences flanking the variable site are also ATs. We have shown in a systematic study of AT sequences that the local conformation of the base-pair segment can modulate long-range transport (27). Analogously, the flexibility intrinsic to TA-rich DNA segments appears to be attenuating long-range charge transport. Indeed, these data point to a greater dynamical flexibility associated with the ATT matched sequence compared even to mismatched ones.

**Correlation with Melting Temperature ( $T_m$ ) Data.** The melting temperatures of DNA duplexes used in a parallel NMR study (18) vary as GC > AT > GG > TT ~ AA > CC (Table 2). These sequences represent the internal 9 bases of the ruthenated assemblies in which long-range oxidative damage was measured. GC and AT base pairs are fully matched Watson-Crick base pairs, and oligonucleotides containing these

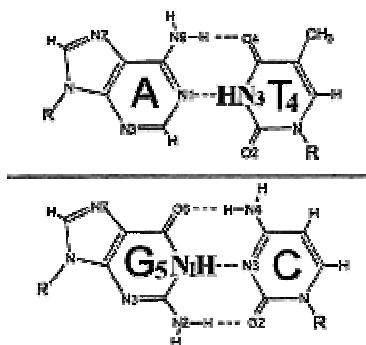
matched pairs display the highest melting temperatures, despite the noteworthy low value for long-range oxidative damage with the matched AT base pair. Thermodynamically, GG and GA mismatches are the most stable of the mismatches, because they are well stacked, given the larger aromatic surface area for purines, and stabilized by hydrogen bonding. The GA mismatch is also known to be well incorporated structurally within the helix (28). The GG mismatch is also well stacked, on the basis of crystallographic and NMR studies, (29) and its presence does not lead to a distortion in the global conformation of the B-form duplex. Correspondingly, these base pairs have fairly high distal/proximal guanine oxidation ratios. AA mismatches have high stacking potential but can form only one hydrogen bond, (30) while TT mismatches have a lower stacking potential but are stabilized by two hydrogen bonds (30). CC is the least stable of the mismatches, as it has a low stacking propensity and is likely stabilized by only one hydrogen bond (31). These characteristics are reflected in the trend of the melting temperatures of the duplexes.

The thermodynamic stabilities of the different mismatches, reflecting in part the local distortion produced, cannot, however, fully account for the varied yield of oxidized products. The striking discrepancy is for the matched AT pair, which shows a high melting temperature but low oxidative damage ratio. Additionally, on the basis of the thermodynamic data alone, TT and AA mismatches should show similar distal/proximal guanine oxidation ratios; however, this is not the case.

**Table 1.2.** Melting Temperatures ( $T_m$ ) and the Base-Pair Lifetimes ( $\tau_{ex}$ ) Based on Measurement of the Imino Proton Exchange at the Mismatch Site ( $X_5$ ) and Its Flanking Bases of the Duplexes Containing Single Intervening Mismatch

Duplexes <sup>a</sup>	$T_m$ (°C) <sup>b</sup>	$\tau_{ex}$ ( $X_5$ NH) (ms) <sup>c</sup>	$\tau_{ex}$ ( $T_6/T_4$ NH) (ms) <sup>c</sup>
5'GACAGTGTC3' 3'CTGTGACAG5'	34.9	$2 \pm 1^e$	$24 \pm 5$
5'GACACTGTC3' 3'CTGTACACAG5'	24.5	$X^d$	$10 \pm 3$
5'GACAATGTC3' 3'CTGTAAACAG5'	32.1	$X^d$	$15 \pm 3$
5'GACATTGTC3' 3'CTGTTACAG5'	32.4	$0.5 \pm 0.3$	$6 \pm 4$
5'GACAGTGTC3' <sup>f</sup> 3'CTGTACACAG5'	47.8	$18 \pm 4$	$12 \pm 3$
5'GACAATGTC3' 3'CTGTTACAG5'	44.1	$1 \pm 0.4$	$8 \pm 2$

<sup>a</sup> These sequences represent the nine internal bases of the ruthenated assemblies in which long-range oxidative damage was measured. <sup>b</sup> Melting temperatures were determined as described in the Experimental Section. <sup>c</sup> Shown are the mean and standard deviation of the base-pair lifetime values of the mismatch and its flanking base pairs based on three trials. The base-pair lifetime values are obtained from imino exchange experiments using <sup>1</sup>H NMR (18). <sup>d</sup> Because only guanine and thymine have imino protons, no base-pair lifetimes are obtained for CC and AA duplexes directly at the corresponding mismatch sites. <sup>e</sup> Two independent values of the base-pair lifetimes at the mismatch site are obtained for the duplex containing GG mismatch for each trial, and these have been averaged. <sup>f</sup> Schematic showing the imino protons ( $T_4N_3H$  &  $G_5N_1H$ ) of the fully matched duplex.



**Correlation with Free Energy of Helix Destabilization.** We also examined the possible correlation between the mean values of distal/proximal guanine oxidation data with free energy data for helix disruption of the same mismatches within the identical (AXT/TYA) sequence context (Figure 5) (32). Overall, significant correlation was observed ( $R = 0.84$ ). Note that these data do not include matched pairs; however, purine-purine mismatches have larger surface areas and can stack well in the helix. Hence, they are not significantly destabilizing. Similarly, they show a high yield of distal guanine oxidation products. Pyrimidine-pyrimidine mismatches have smaller surface areas and tend to destabilize the duplex. These mispairs reasonably show low distal/proximal guanine oxidation ratios.

**Correlation with Electrochemical Data.** Earlier, we had systematically examined the effects of intervening mismatches on the reduction of daunomycin intercalated in DNA-modified electrodes (12). It is interesting to compare the results described here with those seen by electrochemistry. Important differences exist between the two experiments. In the electrochemical measurement, the time scale for the charge transport is much slower,  $10^{-2}$  s, which we ascribed to transport through the extended  $\pi$ -bonded linker. Furthermore, in the electrochemical study, one monitors a reduction reaction rather than an oxidation. Additionally, in the DNA film, the oligomers are closely packed, limiting their flexibility. We attribute the ability to obtain significantly higher relative yields of charge transport using AT-rich sequences in DNA films but not in solution to this constraint on flexibility within the film. Moreover, it has been proposed that the collective properties of these films may substantially alter their charge transport properties (33).

Despite the significant differences in these experiments, there is a clear correlation evident between the electrochemical data and measurements of oxidative damage. Figure 6 shows the plot correlating the two measurements. In fact, for all of the

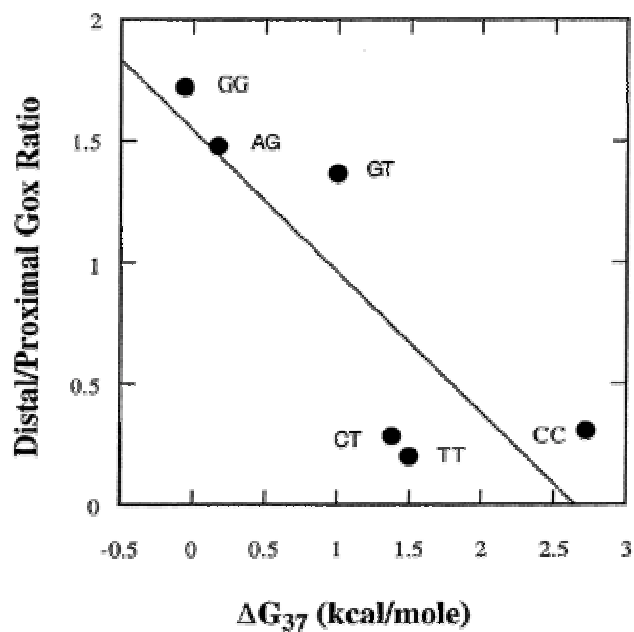


**Figure 1.5.** Correlation plot of the free energies of helix destabilization at 37 °C and the distal/proximal ratios of long-range guanine oxidation in duplexes containing intervening mismatch. The free energy data of the mismatches in the identical sequence context (AXT/TYA) was obtained from the literature (32). A correlation  $R = 0.84$  is observed.

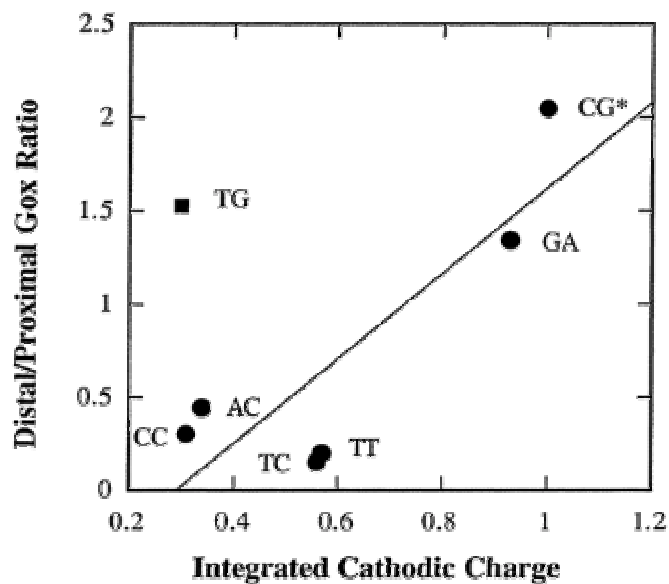


**Figure 1.6.** Correlation plot of the electrochemical data and the distal/proximal ratios of long-range guanine oxidation in duplexes containing intervening mismatch. The integrated background-subtracted cathodic charge passing through the mismatch containing oligonucleotides is obtained from ref 12a and is normalized with respect to the integrated cathodic charge obtained from the fully matched duplex. With the exception of the GT mismatch, the correlation is high (excluding GT,  $R = 0.86$ ).

mismatches with the exception of GT, the correlation is high (excluding GT,  $R = 0.86$ ). Again, note, however, that the matched AT sequence is not included; for all matched sequences, the integrated cathodic charge is high.

Interestingly, in the case of the GT mismatch, the electrochemical data clearly differ from the guanine oxidation data. GT shows a very high distal/proximal oxidation ratio, while the integrated cathodic charge is very small as compared to that for the fully matched sequence. We reconcile this difference on the basis of the difference in time scale for the two experiments. The GT mismatch is known to exist as a wobble pair, well stacked in the helix and stabilized by hydrogen bonding (34). On the fast time scale for long-range oxidative damage ( $\leq 10^{-7}$  s) (35), the mismatched bases are fully stacked in one of the two hydrogen-bonded structures. If, however, the time scale for the wobble is comparable to that for the electrochemical measurement ( $10^{-2}$  s), an attenuation in electrochemical signal should be observed. The dynamics of the wobble pair, therefore, appears to modulate charge transport through this mismatched duplex.

It is also remarkable that, overall, these data show some correlation despite the fact that one is the result of electron transport and the other, hole transport. If the oxidative damage results were considered on their own, one might have invoked the low oxidation potential of guanine being responsible in part for the high overall yield seen with guanine-containing mismatches, and the high oxidation potential for pyrimidines being reflected in their low yields. But purines, even within mismatches, are well-stacked, while pyrimidines less so. It is clearly this feature that dominates the charge transport results for the different single base mismatches.

#### **Correlation with Imino Exchange Rates as a Measure of Base-Pair Lifetimes.**

We have also carried out measurements of the base imino exchange rates using  $^1\text{H}$  NMR to determine the effect of the mismatch on exchange not only at the mismatched base but also at the flanking positions (18). These data are summarized in Table 2. Short base-pair lifetimes ( $\leq 2$  ms) are observed on the basis of imino proton exchange directly at the

mismatch sites as compared to the Watson-Crick GC base pair ( $\epsilon_{\text{ex}}(\text{G}_5\text{NH}) = 18 \text{ ms}$ ). Furthermore, the mismatched site containing guanine, GG, is significantly longer than that of the TT mismatch (0.5 ms). The increased exchange associated with pyrimidine mismatches is evident also from the base-pair lifetime of the adjacent sites, as seen in the  $\text{T}_6\text{NH}$  and  $\text{T}_4\text{NH}$  imino proton exchange. Indeed, exchange in neighboring sites shows that the effects of the mismatch propagates out to neighboring positions. Overall, then, on the basis of the kinetics of imino proton exchange, the duplex containing the GG mismatch displays longer a base-pair lifetime, followed by AA and CC, with TT displaying the shortest lifetime.

These data clearly correlate closely with yields of long-range oxidative damage through intervening mismatches. The TT mismatch has a base-pair lifetime that is approximately four times shorter than that of GG, and also, it shows the lowest yield of oxidized product at the distal guanine doublet. The low yield of oxidized product in the case of the CC mismatch also correlates with the shortened base-pair lifetimes at sites flanking the mismatch; thermodynamically, it is the least stable of the mismatches. The imino protons surrounding the AA mismatch exhibit intermediate base-pair lifetimes, correlating well with its intermediate yield in long-range guanine oxidation.

It is noteworthy that these measurements of imino exchange also reveal a particularly short lifetime for the AT base pair. The AT flanking sequences here are identical to those used in measurements of oxidative damage. No other methodology, besides our measurements of long-range oxidative damage, has revealed a similar diminution compared to purine-purine mismatches. What these NMR and charge transport studies appear to have in common is a sensitivity to base dynamics. These NMR studies, like charge transport studies, also reveal a greater dynamical motion associated with the AT-rich segment.

From these data and their high correlation with measurements of long-range oxidative damage, it is clear that the dynamics of the mismatched base pair and its

flanking sites, rather than overall helical stability, are critical determinants of DNA-mediated charge transport.

**Implications.** Here, we have documented systematically the effects of intervening mismatches on long-range charge transport through DNA. We find DNA-mediated charge transport and the oxidative damage results to be extremely sensitive to the presence of intervening mismatches. This sensitivity may be attributed in part to local changes in helical stability, though these changes cannot be explained through an increased solvent accessibility associated with a mismatch. Similarly, while local changes in the energetics of the DNA bridge occur, these too cannot account for the variations in charge transport that are observed.

Instead, these results underscore the importance of base-pair dynamics in modulating long-range charge transport. While thermodynamic parameters show only a weak correlation with measurements of long range oxidative damage as a function of intervening mismatches, a strong empirical correlation with the base pair and mispair lifetimes is apparent. The time scale for charge transport is clearly much shorter than that for measured imino exchange rates. Transient absorption studies indicate charge transport in the ruthenated duplexes to be  $\leq 10^7 \text{ s}^{-1}$  over  $50 \text{ \AA}$  in well-matched duplexes (35), while the imino protons in these duplexes exchange on the millisecond time scale. Likely, then, the attenuation in yield of damage we observe reflects the relative populations in stacked and destacked orientations on the time scale of the charge transport. It is noteworthy in this context to recall a discrepancy between the electrochemical measurements, also on a slow time scale ( $10^2 \text{ s}^{-1}$ ),<sup>12</sup> and the oxidative damage measurements; a large attenuation in signal is seen for the GT mismatch electrochemically but not in long range oxidative damage. We attribute this difference to the fact that the GT wobble is well stacked in both orientations, allowing charge transport to effect damage in both cases; only when the wobble motion is on the same time scale as the measurement, by electrochemistry, is attenuation observed.

It is likely also that the slow motions yielding imino exchange are correlated themselves with other DNA motions on faster time scales. Unlike solid-state  $\pi$ -stacks, double helical DNA represents a molecular  $\pi$ -stacked array, an array that undergoes dynamical motion on the picosecond-millisecond time scales. Different methods have been utilized to probe the bending, tilting, and twisting of DNA base pairs on these many time scales, and not surprisingly, such motions are perturbed as a result of structural perturbations within the helix (36). Specifically, fluorescence studies have shown variations in base motions in the presence of mismatches on the nanosecond time scale (17) and, as a correlate, NMR studies show variations on the millisecond time scale (18, 28, 30, 31, 34, 37). It is perhaps not surprising then that these different measurements yield similar conclusions. Motions and dynamical changes in structure on all of these time scales also modulate charge transport through DNA. In fact, these results indicate that charge transport through DNA provides a measure of such dynamical motion.

Finally, given the sensitivity of DNA charge transport to the presence of intervening mismatches, one may consider its possible consequences. Surely, DNA charge transport studies, as a measurement of local destacking, provide a completely new diagnostic approach to the detection of mismatches and genetic mutations in DNA. Electrochemical strategies in fact offer a practical strategy to achieve such sensitive mutational assays (13). One might also consider, however, whether such sensitivity is exploited physiologically, in developing strategies within the cell to detect and repair mismatches within the genome (38).

## **Acknowledgment**

We are grateful to the National Institute of Health for the financial support of this work. We also thank M. E. Nunez for technical assistance.

## References

1. Sugiyama, H.; Saito, I. *J. Am. Chem. Soc.* **1996**, *118*, 7063-7068.
2. Hall, D. B.; Holmlin, R. E.; Barton, J. K. *Nature* **1996**, *382*, 731-735.
3. Steenken, S.; Jovanovic, S. V. *J. Am. Chem. Soc.* **1997**, *119*, 617-618.
4. (a) Nunez, M. E.; Rajske, S. R.; Barton, J. K. *Methods Enzymol.* **2000**, *319*, 165-188. (b) Nunez, M. E.; Barton, J. K. *Curr. Opin. Chem. Biol.* **2000**, *4*, 199-206. (c) Baguley, B. C.; LeBret, M. *Biochemistry* **1984**, *23*, 937. (d) Fromherz, P.; Rieger, B. *J. Am. Chem. Soc.* **1986**, *108*, 5361. (e) Holmlin, R. E.; Dandliker, P. J.; Barton, J. K. *Angew. Chem., Int. Ed. Engl.* **1997**, *36*, 2714. (f) Kelley, S. O.; Barton, J. K. *Chem. Biol.* **1997**, *5*, 413. (g) Kelley, S. O.; Barton, J. K. *Science* **1999**, *283*, 375. (h) Kelley, S. O.; Holmlin, R. E.; Stemp, E. D. A.; Barton, J. K. *J. Am. Chem. Soc.* **1997**, *119*, 9861. (i) Lewis, F.; Wu, T.; Zhang, Y.; Letsinger, R.; Greenfield, S.; Wasielewski, M. *Science* **1997**, *277*, 673. (j) Lewis, F.; Wu, T.; Liu, X.; Letsinger, R.; Greenfield, S.; Miller, S.; Wasielewski, M. *J. Am. Chem. Soc.* **2000**, *122*, 2889-2902. (k) Lewis, F.; Liu, X.; Liu, J.; Miller, S.; Hayes, R.; Wasielewski, M. *Nature* **2000**, *406*, 51-53. (l) Manoharan, M.; Tivel, K.; Zhao, M.; Nafisi, K.; Netzel, T. *J. Phys. Chem.* **1995**, *99*, 17461. (m) Murphy, C.; Arkin, M.; Jenkins, Y.; Ghatlia, N.; Bossmann, S.; Turro, N.; Barton, J. K. *Science* **1993**, *262*, 1025. (n) Dandliker, P. J.; Nunez, M. E.; Barton, J. K. *Biochemistry* **1998**, *37*, 6491.
5. Nunez, M. E.; Hall, D. B.; Barton, J. K. *Chem. Biol.* **1999**, *9*, 85.
6. Hall, D. B.; Barton, J. K. *J. Am. Chem. Soc.* **1997**, *119*, 5045.
7. (a) Rajske, S. R.; Kumar, S.; Roberts, R. J.; Barton, J. K. *J. Am. Chem. Soc.* **1999**, *121*, 5615. (b) Rajske, S. R.; Barton, J. K. *J. Biomol. Struct. Dyn.* **2000**, *11*, 285-295.
8. (a) Gasper, S. M.; Schuster, G. B. *J. Am. Chem. Soc.* **1997**, *119*, 12762. (b) Ly, D.; Sani, L.; Schuster, G. B. *J. Am. Chem. Soc.* **1999**, *121*, 9400. (c) Henderson, P. T.; Jones, D.; Hampikian, G.; Kan, Y. Z.; Schuster, G. B. *Proc. Natl. Acad. Sci. U.S.A.* **1999**, *96*, 8353. (d) Schuster, G. B. *Acc. Chem. Res.* **2000**, *33*, 253-260. (e) Meggers, E.; Kusch, D.; Spichty, M.; Wille, U.; Giese, B. *Angew. Chem., Int. Ed. Engl.* **1998**, *37*, 460-462. (f) Giese, B.; Wessely, S.; Spormann, M.; Lindemann, U.; Meggers, E.; Michel-Beyerle, M. E. *Angew. Chem., Int. Ed. Engl.* **1999**, *38*, 996. (g) Meggers, E.; Michel-Beyerle, M. E.; Giese, B. *J. Am. Chem. Soc.* **1998**, *120*, 12950. (h) Giese, B. *Acc. Chem. Res.* **2000**, *33*, 631-636. (i) Saito, I.; Nakamura, T.; Nakatani, K.; Yoshioka, Y.; Yamaguchi, K.; Sugiyama, H. *J. Am. Chem. Soc.* **1998**, *120*, 12686-12687. (j) Nakatani, K.; Sando, S.; Saito, I. *J. Am. Chem. Soc.* **2000**, *122*, 2172-2177. (k) Lewis, F. D.; Letsinger, R. L.; Wasielewski, M. R. *Acc. Chem. Res.* **2001**, *34*, 159-170.
9. Arkin, M. R.; Stemp, E. D. A.; Barton, J. K. *Chem. Biol.* **1997**, *4*, 389.
10. Giese, B.; Wessely, S. *Angew. Chem., Int. Ed. Engl.* **2000**, *39*, 3490.

11. Johnston, D. H.; Glasgow, K. C.; Thorp, H. H. *J. Am. Chem. Soc.* **1995**, *117*, 8933.
12. (a) Kelley, S. O.; Boon, E. M.; Barton, J. K.; Jackson, N. M.; Hill, M. G. *Nucleic Acids Res.* **1999**, *27*, 4830. (b) Kelley, S. O.; Jackson, N. M.; Hill, M. G.; Barton, J. K. *Angew. Chem., Int. Ed. Engl.* **1999**, *38*, 941.
13. Boon, E. M.; Ceres, D. M.; Drummond, T. G.; Hill, M. G.; Barton, J. K. *Nat. Biotechnol.* **2000**, *18*, 1096.
14. Gueron, M.; Leroy, J. L. *Nucleic Acids Mol. Biol.* **1992**, *6*, 1.
15. (a) Leroy, J. L.; Charretier, E.; Kochoyan, M.; Gueron, M. *Biochemistry* **1988**, *27*, 8894-8898. (b) Leijon, M.; Sehlstedt, U.; Neilsen, P. E.; Graslund, A. *J. Mol. Biol.* **1997**, *271*, 438-455. (c) Gueron, M.; Leroy, J. L. *Methods Enzymol.* **1992**, *261*, 383-413.
16. Dornberger, U.; Leijon, M.; Fritzsche, H. *J. Biol. Chem.* **1999**, *274*, 6957-6962.
17. Guest, C. R.; Hochstrasser, R. A.; Sowers, L. C.; Millar, D. P. *Biochemistry* **1991**, *30*, 3271-3279.
18. Bhattacharya, P. K.; Cha, J.; Barton, J. K. *Nucleic Acids Res.* **2002**, *30*, 4740-4750.
19. Caruthers, M. H.; Barone, A. D.; Beaucage, S. L.; Dodds, D. R.; Fisher, E. F.; McBride, L. J.; Matteucci, M.; Stabinsky, Z.; Tang, J. Y. *Methods Enzymol.* **1987**, *154*, 287-313.
20. Anderson, P. A.; Deacon, G. B.; Haarmann, K. H.; Keene, F. R.; Meyer, T. J.; Reitsma, D. A.; Skelton, B. W.; Strouse, G. F.; Thomas, N. C.; Treadway, J. A.; Whit, A. H. *Inorg. Chem.* **1995**, *34*, 6145.
21. Dandliker, P. J.; Holmlin, R. E.; Barton, J. K. *Bioconjugate Chem.* **1999**, *10*, 1122.
22. Dupureur, C. M.; Barton, J. K. *Inorg. Chem.* **1997**, *36*, 33.
23. Sambrook, J.; Fritsch, E. F.; Maniatis, T. *Molecular Cloning: A Laboratory Manual*, 2nd ed.; Cold Spring Harbor Laboratory Press: Cold Spring Harbor, NY, 1989.
24. Stemp, E. D. A.; Arkin, M. R.; Barton, J. K. *J. Am. Chem. Soc.* **1997**, *119*, 2921.
25. Chang, I.; Gray, H. B.; Winkler, J. R. *J. Am. Chem. Soc.* **1991**, *113*, 7056-7057.
26. Barton, J. K. *Science* **1986**, *233*, 727. 27. Williams, T. T.; Odom, D. T.; Barton, J. K. *J. Am. Chem. Soc.* **2000**, *122*, 9048.
28. (a) Brown, T.; Leonard, G. A.; Booth, E. D.; Chambers, J. *J. Mol. Biol.* **1989**, *207*, 455. (b) Maskos, K.; Gunn, B. M.; LeBlanc, D. A.; Morden, K. M. *Biochemistry* **1993**, *32*, 3583-3595. (c) Gao, X.; Patel, D. J. *J. Am. Chem. Soc.* **1988**, *110*, 5178-5182.

29. (a) Skelly, J. V.; Edwards, K. J.; Jenkins, T. C.; Neidle, S. *Proc. Natl. Acad. Sci. U.S.A.* **1993**, *90*, 804. (b) Faibis, V.; Cognet, J. A. H.; Boulard, Y.; Sowers, L. C.; Fazakerley, G. V. *Biochemistry* **1996**, *35*, 14452.
30. Gervais, V.; Cognet, J. A. H.; LeBret, M.; Sowers, L. C.; Fazakerley, G. V. *Eur. J. Biochem.* **1995**, *228*, 279-290.
31. (a) Boulard, Y.; Cognet, J. A. H.; Fazakerley, G. V. *J. Mol. Biol.* **1997**, *268*, 331-347. (b) Peyret, P.; Seneviratne, A.; Allawi, H. T.; SantaLucia, J., Jr. *Biochemistry* **1999**, *38*, 3468-3477.
32. (a) Allawi, H. T.; SantaLucia, J., Jr. *Biochemistry* **1998**, *37*, 9435-9444. (b) Allawi, H. T.; SantaLucia, J., Jr. *Nucleic Acids Res.* **1998**, *26*, 2694-2701. (c) Allawi, H. T.; SantaLucia, J., Jr. *Biochemistry* **1998**, *37*, 2170-2179.
33. Hartwich, G.; Caruana, D. J.; de Lumley-Woodyear, T.; Wu, Y. B.; Campbell, C. N.; Heller, A. *J. Am. Chem. Soc.* **1999**, *121*, 10803-10812.
34. (a) Brown, T.; Kennard, O.; Kneale, G.; Rabinovich, D. *Nature* **1985**, *315*, 604. (b) Allawi, H. T.; SantaLucia, J., Jr. *Nucleic Acids Res.* **1998**, *26*, 4925-4934.
35. Wagenknecht, H. A.; Rajski, S. R.; Pascaly, M.; Stemp, E. D. A.; Barton, J. K. *J. Am. Chem. Soc.* **2001**, *123*, 4400-4407.
36. Murphy, C. J. *Adv. Photochem.* **2001**, *26*, 145-217.
37. (a) Pardi, A.; Morden, K. M.; Patel, D. J. *Biochemistry* **1982**, *21*, 6567-6574. (b) Patel, D. J.; Kozlowski, S. A.; Ikuta, S.; Itakura, K. *Biochemistry* **1984**, *23*, 3207-3217. (c) Patel, D. J.; Kozlowski, S. A.; Ikuta, S.; Itakura, K. *Fed. Proc.* **1984**, *43*, 2663-2670. (d) Moe, J. G.; Russu, I. M. *Biochemistry* **1992**, *31*, 8421-8428.
38. Rajski, S. R.; Jackson, B. A.; Barton, J. K. *Mutat. Res.* **2000**, *447*, 49-72.